OPEN ACCESS
Freely Available Online

OpenAccessPub

Neurological Research and Therapy
ISSN NO: 2470-5020

Research Article

DOI : 10.14302/issn.2470-5020.jnrt-16-993

Skeletal Muscle Calcium Channel Mutation R528G: Enhanced Channel Inactivation and Omega-Current at Hyperpolarization Contribute to Hypokalemic Periodic Paralysis.

Marcin Bednarz[1]*,*, Yuwei Da[2]*,*, Frank Lehmann-Horn[1], Chunxiang Fan[1], Jens Schallner[3], Karin Jurkat-Rott[1,*]

1. Division of Neurophysiology, Ulm University, Albert-Einstein-Allee 11, 89081 Ulm, Germany
2. Department of Neurology, Xuan Wu Hospital, Capital Medical University, Beijing 100053, China
3. Clinic and Polyclinic for Children and Youth Medicine, Neuropaediatrics, University Clinic Carl Gustav Carus 01304 Dresden, Germany

*,*contributed equally

Abstract

Autosomal dominant inherited hypokalemic periodic paralysis (HypoPP) is caused by S4 voltage sensor mutations in skeletal muscle $Ca_V1.1$ calcium or $Na_V1.4$ sodium channels. In the present study, a small German family with the known $Ca_V1.1$-R528G is described. The phenotype consists of short and infrequent episodes of limb weakness with ictal respiratory and cardiac involvement. There is incomplete penetrance in women, and acetazolamide is beneficial in two patients also taking daily potassium. Expression of the mutation in the GLT mouse muscle cell line revealed accelerated kinetics of inactivation by twofold, a left-shift of the steady-state inactivation curve by 13mV and a reduced recovery from fast inactivation by up to 39%. These changes suggest a stabilization of the inactivated state. Additional significant slowing of activation may support a second open state with differing ion selectivity or decreased activation of calcium-activated potassium channels and thereby contribute to weakness similar to other $Ca_V1.1$ mutations. Also, as documented for other HypoPP mutants, we found a hyperpolarization-induced inward guanidinium current of 22nS/nF which can be interpreted as an omega current along the voltage sensor gating pore that leads to a gain- of- function at potentials near the resting membrane potential. This finding can explain the long-lasting depolarizations that are known to lead to paralysis. The omega current is large enough so that a relatively mild hypokalemic trigger of 2.4mM already produces episodes of weakness *in vivo*.

Corresponding author: Karin Jurkat-Rott, Division of Neurophysiology, Ulm University, Albert-Einstein-Allee 11, 89081 Ulm, Tel:+49 731 500 23251, Fax:+49 731 500 23260

Academic Editor: Zheng Jiang, Johns Hopkins University School of Medicine
Citation: Marcin Bednarz, Yuwei Da, Frank Lehmann-Horn, Chunxiang Fan, Jens Schallner et al. (2016) Skeletal Muscle Calcium Channel Mutation R528G: Enhanced Channel Inactivation and Omega-Current at Hyperpolarization Contribute to Hypokalemic Periodic Paralysis. . Journal of Neurological Research And Therapy - 1(3):20-30. https://doi.org/10.14302/issn.2470-5020.jnrt-16-993

Running title: $Ca_V1.1$-R528G
Key words: skeletal muscle calcium channel, $Ca_V1.1$, omega current, hypokalemic periodic paralysis, HypoPP, acetazolamide, CACNA1S, R528G, GLT, myotubes
Received : Mar 30, 2016; **Accepted** : Jun 06, 2016; **Published** : Jun 10, 2016;

Introduction

Familial hypokalemic periodic paralysis (HypoPP) is an autosomal dominant disorder of the skeletal muscle. It is characterized by episodes of generalized paralysis caused by reduced serum potassium. Additional permanent weakness and myopathy occurs in 68% of patients (1). Two genes of voltage-gated cation channels are genetically causative, CACNA1S coding for $Ca_V1.1$ (HypoPP-1) and SCN4A encoding $Na_V1.4$ (HypoPP -2). The $Ca_V1.1$ Ca^{2+} channel serves both as ion-conducting pore and as voltage sensor for excitation-contraction coupling while $Na_V1.4$ initiates the action potential. Almost all mutations are located in the voltage -sensing transmembrane segment S4 and replace arginine residues occurring at every third position (reviewed in 2,3,4). Glycine mutations generally reduce treatment response to the standard medication acetazolamide (5).

Pathogenetically, a long-lasting membrane depolarization is responsible for the paralysis episodes and has been shown to be caused by an aberrant omega current that flows through the S4 mutation gating pore instead of the central ion-conducting alpha pore of the channel (originally described in 6,7). Depending on the location of the mutated residue, the voltage range in which the omega current occurs differs because S4 segments move outward during channel activation. Briefly, the more inward the mutation the more depolarized the voltage range; therefore, the outermost mutations conduct omega currents at hyperpolarized potentials when the central alpha pore is closed (reviewed in 2,3,4). Also, the size of the residue replacing arginine influences the size of the omega current suggesting arginine-to-glycine mutations to generate the largest omega currents and therefore the most severe phenotypes (reviewed in 8).

Even though almost all HypoPP functional studies have been done on $Na_V1.4$ mutations, $Ca_V1.1$ mutations are much more abundant and explain up to 77% of patients with hereditary HypoPP (9) with the most frequent being R528H and R1239H (10). It has not been systematically shown that the conclusions drawn for $Na_V1.4$ are applicable to $Ca_V1.1$. Until now, there is only circumstantial evidence for omega currents of R1239H in native muscle of patients (11) and measurements of omega current of R528 in native muscle of transgenic mice (12). Additionally, our group detected omega currents using a mouse cell line expressing R1242G-$Ca_V1.1$ which is, however, associated to normokalemic periodic paralysis with transient compartment-like syndrome (13). For several other mutations in $Ca_V1.1$, omega currents and alpha pore currents have not yet been studied.

In this work, we study the R528G mutation in domain II of $Ca_V1.1$ for which neither omega current nor alpha pore current has been examined. It has been reported in a one large HypoPP family (14) and as a de novo mutation in a single patient (15). In this study we found it in a small German family. Based on the current model of pathogenesis, we would expect i) a more severe phenotype, ii) a bad response to acetazolamide and iii) a large omega current in the range of the resting membrane potential as pathogenetic mechanism. We test these hypotheses and additionally examine alpha pore currents to discuss their possible contribution to the phenotype.

Patients and Methods

Patients :

Clinical and genetic examination was approved of by the institutional review board of Ulm and conducted according to the declaration of Helsinki. Blood was taken with informed consent from the proband, his brother, mother, and aunt. His mother sent blood but did not wish to be examined otherwise. Exons 11 and 30 of CACNA1S were studied for routine diagnosis using Sanger sequencing.

Mutagenesis :

Rabbit cDNA in a PSG5 vector (Stratagene) containing pGFP37 was employed for site-directed mutagenesis (13). The C1582G cDNA mutation which results in the R528G amino acid change was introduced using PCR-based site-directed mutagenesis with the reverse oligonucleotide 5′-CGGATGCAGTGCAACACGG-3′ (Eurofins MWG GmbH, Ebersberg) and verified by Sanger sequencing. Heterologously expressed rabbit cDNA of $Ca_V1.1$ in GLT cells produces larger currents with otherwise equivalent gating parameters to human cDNA as shown previously (16).

Cell Culture and Transfection:

Myotubes of the homozygous dysgenic cell line GLT were cultured as previously described (13,16,17). Briefly, GLT cells were cultured in a growth medium consisting of 80% Dulbecco's modified Eagle medium, 10% fetal bovine serum, and 10% horse serum (HS), 1% Glutamate (all Gibco) in sterile flasks or gelatine-coated dishes. Serum content was reduced to fusion medium containing only 2% HS, on day 1 after the last passaging procedure to induce maturation and fusion of cells in the dishes. Transfection was performed with 4µg FugeneHD (Roche) reagent to 2µg cDNA on cells, two days after first use of fusion medium.

Electrophysiology:

Standard whole-cell recordings were performed on 7-9 days old myotubes. Series resistance was partially (30-60%) compensated by the analog circuitry of the Axopatch 200B patch-clamp amplifier (Axon Instruments), with voltage errors less than 5 mV. Before acquiring data, individual cells were allowed to equilibrate for 5min after achieving internal access. For alpha pore current experiments, the bathing solution contained (in mM): TEA-Cl 132, $CaCl_2$ 10, $MgCl_2$ 1, HEPES 10, glucose 5, 4-aminopyridine (4-AP) 2.5, tetrodotoxin 0.005 (pH 7.4). Pipettes were filled with (in mM): CsCl 128, HEPES 12, EGTA 10, Mg-ATP 5, phosphocreatine 5 (pH 7.2). For omega current measurements, the bathing solution contained (in mM): TEA-methanesulfonate (MS) 80, Guanidinium sulfate 38, $MgSO_4$ 1, Ca-gluconate 5, Glucose 5, 4-aminopyridine (4 -AP) 2.5, HEPES 10 (pH 7.4). Pipettes were filled with (in mM): TEA-MS 65, Cs-MS 65, EGTA 10, MgATP 5, $Na_2CreatinPO_4$ 5, HEPES 12 (pH 7.2). All measurements were performed at room temperature (20-25°C). Data were filtered at 1kHz and sampled at 2kHz. Each experiment was performed on six to ten cells.

Pulse Protocols for Alpha Currents:

To elicit whole-cell Ca^{2+} currents, a series of 600ms pulses from -60mV to 50mV in 5mV steps from a holding potential of -90mV were performed. Steady-state activation parameters were determined by fitting the current-voltage relation with the equation $I=G_{leak}*(V-V_{leak})+G_{max}*(V-V_{rev})/(1+\exp((V_{0.5}-V)/k))$, where G_{leak} and V_{leak} respectively are the conductance and reversal potential of the linear leak, G_{max} and V_{rev} respectively are maximum conductance and reversal potential of the alpha pore current $V_{0.5}$ and V respectively are the potential for the half-maximal current and the test potential, and k is the slope factor. The kinetics of activation was estimated by fitting the activation time course to a single exponential function as $I=\exp(-t/\tau_{act})+C$ and plotting the time constant of activation (τ_{act}) as a function of the test voltage ranging between +10mV and +50mV. To avoid interference by a residual capacitive transient, we began the fits 8ms after the start of the test pulse.

For the examination of the steady-state activation, cells were held at -90mV and then depolarized by a series of 60s prepulses from -90mV to +30mV in 10mV increments prior to a test pulse of 30mV. The peak Ca^{2+} current measured during the test pulse was plotted as a function of conditioning voltage for both WT and R528G channels (Figure 1C). Boltzmann functions were fitted to the data of the WT

Figure 1. $Ca_V1.1$ alpha pore currents in GLT myotubes

Original traces of calcium alpha pore currents from heterologously expressed wild-type (A) and R528G (B) channels in GLT myotubes. (C) Conductance-voltage relationship from Bolzmann fits of steady-state activation and inactivation. Note the left shift of inactivation of the mutant. (D) Kinetcs of activation and (E) inactivation determined by monoexponentional fits. Note the slowed activation and accelerated inactivation of the mutant. (F) Recovery from fast inactivation as determined by a single exponential fit. Note the incomplete recovery of the mutant. All error bars represent the mean ± SEM. The p values are *<0.05; **<0.01 and ***<0.001.

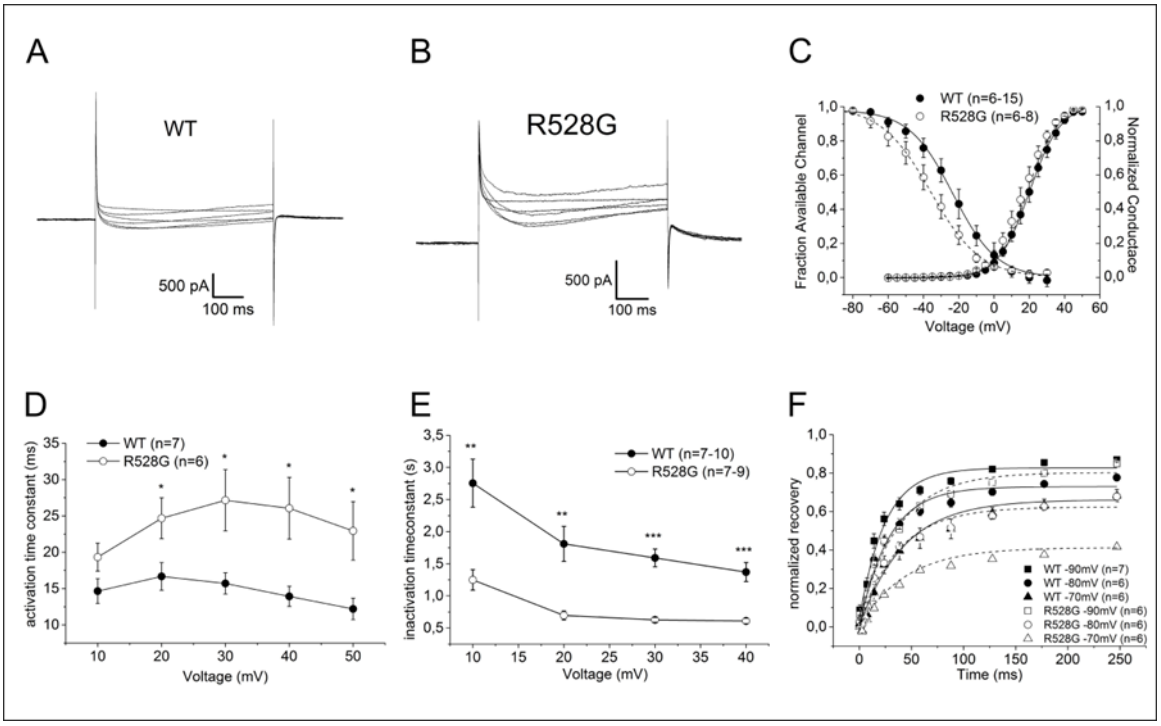

and mutant channels by the equation $I/I_{max}=A/(1+\exp((V_{0.5}-V)/k))+C$, where A represents the fraction of inactivated channels, V is the pre-pulse potential, $V_{0.5}$ is the potential at which half of the channels are inactivated, C is the fraction of non-activated channels and k is the slope factor. The time constant of inactivation (τ_h) was determined by fitting a single exponential function to the decaying part of the calcium currents as $I=\exp(-t/\tau_h)+C$ and τ_h values were also plotted as a function of voltage.

The rate of recovery from inactivation at hyperpolarized voltages (-90mV, -80mV or -70mV) was measured by employing a double pulse protocol with varying intermediate repolarization times. Generally, an inactivating 20s prepulse to 30mV was followed by a 300ms test pulse to the same potential. The peak I_{ca} was normalized to the peak current amplitude measured during the prepulse. Test currents were recorded in both WT and R528G cells after recovery intervals ranging from 0.2ms to 247ms at -90mV, -80mV and -70mV. The recovery from fast inactivation was analyzed by fitting the data to a single exponential function, $I/I_{max}=A*(1-\exp(-t/\tau))+C$, where A is the fractional amplitude, τ is the time constant, and C is the level of non-inactivating sodium current.

Pulse Protocol for Omega Currents:

The voltage dependence of omega currents was determined using 10mV steps from -140mV to 0mV over

a period of 200ms from a holding potential of -90mV using solutions containing guanidinium ions. The linear leak was subtracted offline and calculated from a linear fitting curve between -40mV and 0mV using a linear fitting curve y=m*x+b between -40mV and 0mV. After leak subtraction, the current densities (mean current amplitudes divided by cell capacitance) were plotted against the eliciting voltage step. Omega currents were then determined by subtraction of currents from untransfected cells (unspecific background currents) from both WT and mutant currents for comparison.

Statistics:

Whole-cell recordings were analyzed by a combination of pClamp (Axon Instruments), Excel (Microsoft) and ORIGIN (Microcal software, Northampton, MA) programs. Data are presented as mean± SEM, which is shown as bars. Student's double-sided t-test was applied for equal variances or Welch t-test for unequal variances and unequal sample sizes. The significance level was set with *p<0.05, **p<0.01, ***p<0.001 and ****p<0.0001.

Results

Patients:

All 4 samples of the family members we investigated, contained C1582G in CACNA1S, which codes for R528G in $Ca_V1.1$. The proband was referred because of tetraplegia with ictal bradycardia and a serum potassium level of 2.1mM at age 16. In addition to chronic recurrent myalgia, cramping and muscular weakness in the morning hours, the proband suffered from episodic incomplete paresis in the proximal muscle groups of the upper and lower extremities which decreased within hours. To treat a mild muscle weakness after exercise, he prophylactically takes oral potassium. No serious paralysis episodes have occurred after administering acetazolamide 250mg daily. Chronic muscle weakness has not present up to his current age of 26.

The proband's younger brother reported that since approximately 3/4 of a year (onset at age 16), very occasionally a light paresis in the upper arm appears which he noted after prolonged exercise, especially in the evening hours. He takes no acetazolamide, but just lays down for sleep and the next morning it´s all gone. There is no chronic muscle weakness or any further symptoms especially in any facial or pharyngeal muscles.

The proband's aunt had her first episode at age four and reported ictal cardiac arrhythmia. Her episodes of limb paralysis were rare, i.e. detected more or less yearly and lasted for minutes to hours. She also suffered from frequent painful muscle cramping. Her treatment was a combination of daily potassium supplementation plus 250mg acetazolamide. In contrast, the proband's mother (sister of the aunt) reported herself to be unaffected, i.e. not having episodic or chronic weakness. She did not agree to a physical examination or provide any further information.

Functional Expression Levels:

Successfully transfected cells were indicated by GFP fluorescence marking. Since measuring fluorescent density of the very variably shaped, multi-nuclear GLT myotubes was not reliable, maximal conductance, G_{max} (as defined by the formula in the methods section) was used as an indicator of the amount of expressed channels instead. This is a common practice since the GLT cell line does not express endogenous, functional $Ca_V1.1$ (17) and therefore, all alpha pore currents are due to plasmid expression. The G_{max} values as indicated in Table 1 showed no significant difference between WT and mutant. Therefore, we considered their expression levels to be similar.

Alpha Pore Current Activation:

Figure 1 shows original traces of representative calcium alpha pore currents recorded from GLT cells expressing WT (Figure 1A) or R528G (Figure 1B) mutant calcium channels. Both WT and R528G channels showed

Table 1. Parameters of calcium alpha pore currents

	WT	R528G	p
Current activation			
G_{max} (pA/mV)	23.34 ± 2.23	29.85± 8.53	0.48
V_{rev} (mV)	84.06 ± 4.24	78.93 ± 4.63	0.42
$V_{0.5}$ (mV)	20.25 ± 1.94	16.51 ± 2.52	0.26
k (mV)	7.51 ± 0.34	7.46 ± 0.58	0.94
Maximum current density (pA/pF)	5.04 ± 1.17	7 ± 1.94	0.41
n	15	8	
Activation time-constant (τ_a)			
0 (mV)	10.28 ± 1.23	13.14 ± 1.5	0.16
10 (mV)	14.66 ± 1.72	19.32 ± 1.92	0.1
20 (mV)	16.68 ± 1.9	24.68 ± 2.81*	0.03
30 (mV)	15.71 ± 1.46	27.15 ± 4.22*	0.02
40 (mV)	13.93 ± 1.38	26.06 ± 4.25*	0.01
50 (mV)	12.2 ± 1.47	22.94 ± 4.02*	0.02
n	7	6	
Inactivation time-constant (τ_h)			
10 (mV)	2.75 ± 0.37	1.25 ± 0.16**	0.0012
20 (mV)	1.81 ± 0.27	0.70 ± 0.07**	0.0019
30 (mV)	1.59 ± 0.14	0.63 ± 0.04****	0.000002
40 (mV)	1.37 ± 0.15	0.61 ± 0.04***	0.00076
n	7	6	
Steady-state inactivation			
A	0.97 ± 0.01	0.99 ± 0.01	0.12
$V_{0.5}$ (mV)	-23.33 ± 3.66	-36.98 ± 4.71*	0.045
k (mV)	-11.45 ± 1.27	-12.59 ± 0.71	0.45
c	0.01 ± 0.01	0.01 ± 0.01	0.95
n	6	6	
Recovery from inactivation			
-90mV			
A	0.79 ± 0.03	0.78 ± 0.04	0.8
τ_1 (ms)	26.05 ± 2.93	39.44 ± 6.21	0.06
c	0.06 ± 0.02	0.05 ± 0.03	0.91
n	7	6	
-80 mV			
A	0.74 ± 0.02	0.61 ± 0.02**	0.003
τ_1 (ms)	29.69 ± 3.67	40.72 ± 6.52	0.17
c	0.01 ± 0.01	0.03 ± 0.02	0.33
n	6	6	
-70mV			
A	0.69 ± 0.02	0.42 ± 0.06**	0.002
τ_1 (ms)	52.13 ± 15.91	49.67 ± 9.26	0.9
c	0.01 ± 0.01	0.01 ± 0.01	0.89
n	6	6	

*indicates a significant difference between WT and R528G (*p<0.05; **p<0.01; ***p<0.001; ****p<0.0001).

similar current density (Table 1). The parameters of the Boltzmann fits for steady-state activation revealed

similar midpoints ($V_{0.5}$=16.51±2.52mV for R528G *vs.* 20.25±1.94mV for WT) and similar steepness (k=7±1.94mV *vs.* 5.04±1.17 mV; Figure 1C). Therefore, the voltage-dependent activation of the mutant was comparable to wildtype. In contrast, there was an indication of a change of the kinetics of activation. Figure 1D shows the voltage dependence of τ_{act} of WT and R528G. Even though the voltage dependence of τ_{act} of the R528G currents had an overall similar trend to wildtype, significant differences in τ_{act} were present in voltages of +20mV to +50mV, indicating that the R528G mutation slowed the activation rate of the channel at more depolarized potentials.

Alpha Pore Current Inactivation:

R528G showed a 13.65mV hyperpolarizing shift of the steady-state inactivation curve namely $V_{0.5}$ = -36.98±4.71mV *vs.* -23.33±3.66mV (p=0.045), but there was no difference in the steepness between WT and R528G, with k= -12.59±0.71mV *vs.* -11.45±1.27mV (p=0.45; n=6 each). This facilitated inactivation suggested reduced channel function. Additionally, the time constant of inactivation τ_h was markedly faster in the mutant channel than in WT. In the WT channel, τ_h decreased steeply between +10mV and +20mV, a range over which the τ_h value of the mutant was nearly constant. The τ_h values of R528G were significantly smaller than the WT values at all measured voltages (Table 1), namely 1.25±0.16ms *vs.* 2.75±0.37ms (10mV; p<0.0012), 0.70±0.07ms *vs.* 1.81±0.27ms (20mV; p<0.0019), 0.63±0.04ms *vs.* 1.59±0.14ms (30mV; p<0.000002) and 0.61±0.04ms *vs.* 1.37±0.15ms (40mV;p<0.00076) which also suggested a reduced alpha pore current of the mutant.

Alpha Pore Current Recovery from Inactivation: The mutant considerably altered the time course of channel recovery from inactivation at the recovery potentials of -70mV and -80mV (Figure 1F). The fractional amplitude A was lower in the mutant than in the WT channels indicating that the amount of recovering channels is significantly lower (0.61±0.02 *vs.* 0.74±0.02 at -80mV with p<0.003 for n=6; 0.42±0.06 *vs.* 0.69±0.02 at -70mV with p<0.002 for n=6; Figure 1F, Table 1). However, the time constant was not significantly altered at any of the holding potentials. The accelerated rate of inactivation and incomplete recovery from inactivation at -80mV and -70mV indicated a stabilization of the inactivated state of the mutant which was consistent with the left shift of the steady-state inactivation. Taken together, our data clearly demonstrated that the R528G mutation is a hypomorphic mutation and reduces the alpha pore current of the skeletal calcium channel.

Omega Currents:

We found a hyperpolarization-induced inward current of the R528G mutant that was significantly higher than that of the wild-type channels and untransfected cells (Figure 2A) namely -2.57±0.28pA/pF *vs.* -1.59±0.27pA/pF (-140mV); -1.81±0.21pA/pF *vs.* -1.08±0.09pA/pF (-130mV); -1.32±0.2pA/pF *vs.* -0.73 ±0.16pA/pF (-120mV); -1.11±0.24pA/pF *vs.* -0.46±0.08pA/pF (-110mV) and -0.66±0.13pA/pF *vs.* -0.32±0.06pA/pF (-100mV) with p<0.05 and n=7. To characterize it properly, we subtracted the currents of untransfected cells (endogenous background currents) from mutant and WT currents. The resulting current for WT was linear and interpreted to be a background leak current, whereas the resulting current of the mutant was an exponentially decreasing voltage-dependent current comparable to previously described omega currents in a $Ca_V1.1$ HypoPP mutant (13). This omega current had a maximal conductance of 22.17nS/nF (Figure 2B).

Discussion

Comparison of Clinical Features of $Ca_V1.1$ R528 Mutants:

Three $Ca_V1.1$ R528 mutations have been described clinically in the literature: R528H/G/C. An overview is given in Table 2, which includes the data of

our patients (1,5,10,11,14,15,18,19,20). The age of onset for all mutations is approximately the 2nd decade, although the disease manifested slightly earlier in our some support for more severe weakness, the phenotype of R528G cannot be clearly interpreted as more severe than the R528H phenotype.

Figure 2. Omega currents of $Ca_V1.1$ in GLT myotubes

Original traces of guanidinium omega currents from heterologously expressed (A) wild-type and (B) R528G channels and their calculated current densities (C) with additional untransfected GLT myotubes with usual guanidinium solution. (D) Plot of WT minus untransfected vs. mutant minus untransfected from C, fitted with a linear or exponential function. Dashed line indicates a maximal conductance of 22.17nS/nF of the mutant. All error bars represent the mean ± SEM. The p values are *<0.05.

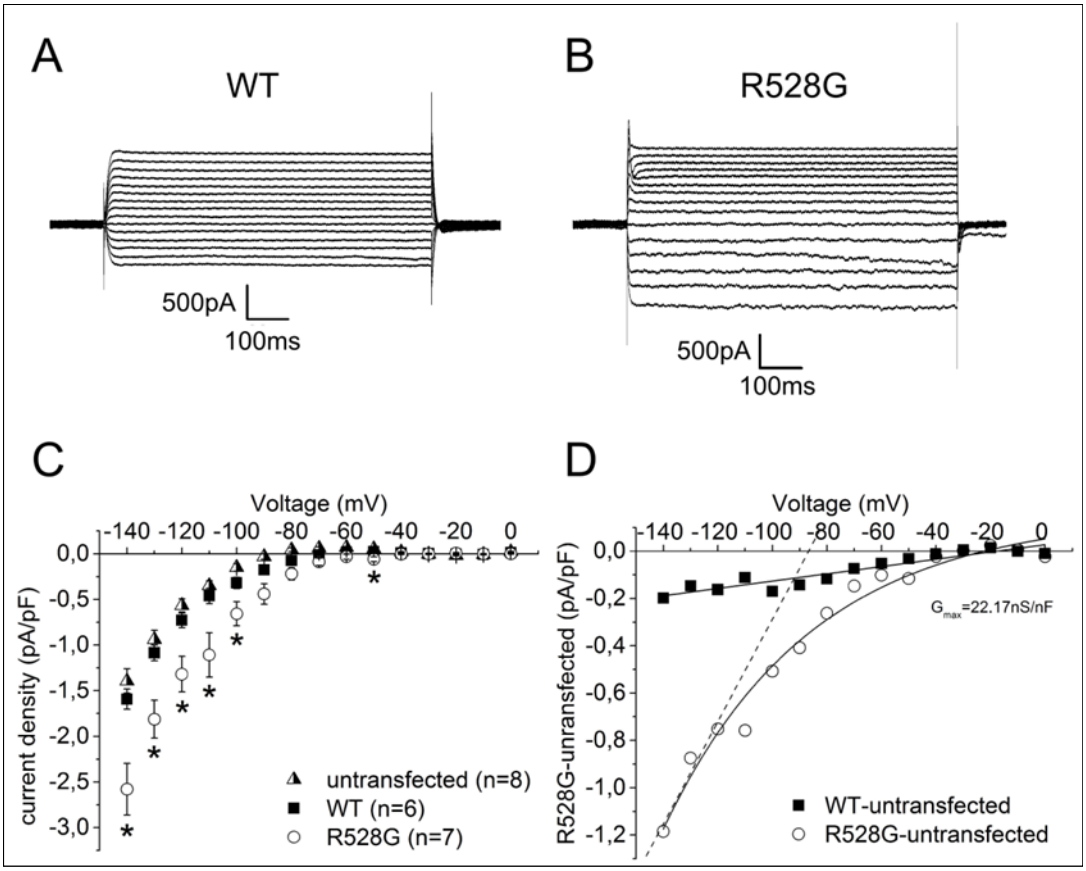

R528G family. Contrary to expectations, R528G/C caused less frequent episodes of shorter duration than did R528H; however, in R528G patients ictal respiratory insufficiency (15) and cardiac involvement (our family) may imply greater severity of the weakness. Still, incomplete penetrance in women was observed for R528G (the proband's mother and reference 14) just as in R528H (10). Unlike the R528H cases, no permanent weakness or vacuolar myopathy has been described in R528C/G patients, but this could be due to the small number of known patients. Therefore, although there is

Triggering factors are similar for all mutations; however, the hypokalemia trigger is milder in R528G patients, which suggests that the omega current must be larger to be able to produce symptoms at higher potassium levels. In contrast to R528H patients for whom acetazolamide regularly ameliorates symptoms, such treatment for R528G patients was only beneficial when combined with daily potassium (our family), but not when administered alone as prophylactic measure (15). The previous studies suggesting that patients with the arginine-to-glycine mutation do not experience any

Table 2. Clinical features of $Ca_V1.1$ R528 mutations.

	R528H	R528G		R528C
		our cases	literature	
age at onset	15	12	16.5	23
frequency of episodes	weekly – monthly	yearly	weekly to monthly	monthly-yearly
duration of episodes	hours	minutes to hours	hours to months	minutes to hours
triggering factors	carbohydrate rich meals, rest after exercise	exercise or stress	carbohydrate rich meals, rest after exercise	exercise or stress
ictal K^+	2mmol/l	2.1mmol/l	2.5mmol/l	1.89mmol/l
therapy with acetazolamide	effective acetazolamide	acetazolamide with daily potassium	acetazolamide ineffective or not described	Not described
weakness	vacuolar myopathy, myopatic changes, proximal legs	weak in upper limbs, recurrent mild attacks	generalized, respiratory insufficiency	weak in right tights than in all limbs
permanent weakness	in 25% of patients	none	not described	not described
penetrance	reduced in women	incomplete	reduced in women	complete

benefit from acetazolamide (5) cannot be fully confirmed because of our family. However, the milder hypokalemic trigger observed in all cases would be in agreement with a larger underlying omega current of R528G compared with R528H.

Alpha Pore Currents:

The slowing of the activation of R528G alpha pore currents is similar to that of the previously characterized mutant R528H (21). The fact that the activation became progressively slower relative to WT with increasing depolarization may indicate an increasing probability for a second open state. R528H showed such a second open state (called O_2) that is more favored in the mutant than in the WT (22). Depending on the ion selectivity of O_2, this state could result in an increased depolarization tendency and thereby inactivation of the action potential-generating Na^+ channels. Additionally, a reduction in the Ca^{2+} current density or delay in the activation of the channel during activity might also disrupt the ability of calcium-activated potassium channels to rescue the muscle cell after a series of action potentials, leading to depolarization and failure of conduction (21) thus contributing to the weakness.

The left shift of the steady-state inactivation is a recurrent finding for $Ca_V1.1$ mutations, i.e., R1242G (13) and R528H (16). Combined with accelerated inactivation and incomplete recovery in R528G, this finding indicates a stabilization of the fast inactivated state and an overall reduced alpha pore current. This would be compatible with permanent weakness which surprisingly was not found clinically. The question arises whether the stabilized inactivated stated limits the duration of weakness episodes because the S4 segment is moved outward in the inactivated state which would shift the residue 528 outside of the gating pore constriction

thereby terminating the omega current.

Omega currents:

Our voltage-clamp measurements of R528G channels expressed in GLT cells revealed a voltage-dependent inward current activated by hyperpolarization with the maximal conductance of 22.17nS/nF in our GLT expression system. Using the same method in form of a linear fit through the inward current at the voltages between -140mV and -120mV, homozygous $Ca_V1.1$ $R528H^{m/m}$ fibers had maximal omega currents of 28nS/nF (12). Because of the different expression systems used, we cannot directly conclude whether the omega current of R528G is actually larger or smaller than that of R528H, however the general magnitude range is similar.

Conclusion

Our data did not confirm the three starting hypotheses because i) the phenotype was not clearly more severe for R528G than for R528H, ii) acetazolamide ameliorated symptoms in combination with daily potassium administration and iii) the omega current for R528G was not larger than for R528H. However, our data confirms that a large omega current is present in the resting potential range which is in agreement with current pathogenetic models of HypoPP (8).

Acknowledgements

This study was supported by the Else-Kröner Fresenius Foundation, the IonNeurONet of the German Federal Ministry of Research BMBF, the German Muscle Disease Society DGB and the non-profit Hertie Foundation.

References

1. Cavel-Greant D, Lehmann-Horn F, Jurkat-Rott K. The impact of permanent muscle weakness on quality of life in periodic paralysis: a survey of 66 patients. (2012) Acta Myol. 31(2):126–33.
2. Cannon SC. Channelopathies of skeletal muscle excitability. (2015) Compr Physiol. 5(2):761–90.
3. Suetterlin K, Männikkö R, Hanna MG. Muscle channelopathies: recent advances in genetics, pathophysiology and therapy. (2014) Curr Opin Neurol. 27(5):583–90.
4. Catterall WA. Signaling complexes of voltage-gated sodium and calcium channels. (2010) Neurosci Lett. 486(2):107–16.
5. Matthews E, Portaro S, Ke Q, Sud R, Haworth A, et al. Acetazolamide efficacy in hypokalemic periodic paralysis and the predictive role of genotype. (2011) Neurology 77(22):1960–4.
6. Sokolov S, Scheuer T, Catterall WA. Gating pore current in an inherited ion channelopathy. (2007) Nature. 446(7131):76–8.
7. Struyk AF, Cannon SC. A Na+ channel mutation linked to hypokalemic periodic paralysis exposes a proton-selective gating pore. (2007) J Gen Physiol. 130(1):11–20.
8. Jurkat-Rott K, Groome J, Lehmann-Horn F. Pathophysiological role of omega pore current in channelopathies. (2012) Front Pharmacol. 3:112.
9. Matthews E, Labrum R, Sweeney MG, Sud R, Haworth A, et al. Voltage sensor charge loss accounts for most cases of hypokalemic periodic paralysis. (2009) Neurology 72(18):1544–7.
10. Elbaz A, Vale-Santos J, Jurkat-Rott K, Lapie P, Ophoff RA, et al. Hypokalemic periodic paralysis and the dihydropyridine receptor (CACNL1A3): genotype/phenotype correlations for two predominant mutations and evidence for the absence of a founder effect in 16 caucasian families. (1995) Am J Hum Genet. 56(2):374–80.
11. Jurkat-Rott K, Weber M-A, Fauler M, Guo X-H, Holzherr BD, et al. K+-dependent paradoxical membrane depolarization and Na+ overload, major and reversible contributors to weakness by ion channel leaks. (2009) Proc Natl Acad Sci U S A. 106

(10):4036–41.

12. Wu F, Mi W, Hernández-Ochoa EO, Burns DK, Fu Y, et al. A calcium channel mutant mouse model of hypokalemic periodic paralysis. (2012) J Clin Invest 122(12):4580–91.
13. Fan C, Lehmann-Horn F, Weber M-A, Bednarz M, Groome JR, et al. Transient compartment-like syndrome and normokalaemic periodic paralysis due to a Ca(v)1.1 mutation. (2013) Brain. 136(Pt 12):3775–86.
14. Wang Q, Liu M, Xu C, Tang Z, Liao Y, et al. Novel CACNA1S mutation causes autosomal dominant hypokalemic periodic paralysis in a Chinese family. J (2005) Mol Med (Berl). 83(3):203–8.
15. Kil T-H, Kim J-B. Severe respiratory phenotype caused by a de novo Arg528Gly mutation in the CACNA1S gene in a patient with hypokalemic periodic paralysis. (2010) Eur J Paediatr Neurol. 14 (3):278–81.
16. Jurkat-Rott K, Uetz U, Pika-Hartlaub U, Powell J, Fontaine B, et al. Calcium currents and transients of native and heterologously expressed mutant skeletal muscle DHP receptor alpha1 subunits (R528H). (1998) FEBS Lett. 423(2):198–204.
17. Powell JA, Petherbridge L, Flucher BE. Formation of triads without the dihydropyridine receptor alpha subunits in cell lines from dysgenic skeletal muscle. (1996) J Cell Biol. 134(2):375–87.
18. Yang B, Yang Y, Tu W, Shen Y, Dong Q. A rare case of unilateral adrenal hyperplasia accompanied by hypokalaemic periodic paralysis caused by a novel dominant mutation in CACNA1S: features and prognosis after adrenalectomy. (2014) BMC Urol. 14:96.
19. Sternberg D, Maisonobe T, Jurkat-Rott K, Nicole S, Launay E, et al. Hypokalaemic periodic paralysis type 2 caused by mutations at codon 672 in the muscle sodium channel gene SCN4A. (2001) Brain. 124(Pt 6):1091–9.
20. Miller TM, Dias da Silva MR, Miller HA, Kwiecinski H, Mendell JR, et al. Correlating phenotype and genotype in the periodic paralyses. (2004) Neurology. 63(9):1647–55.
21. Morrill JA, Brown RH, Cannon SC. Gating of the L-type Ca channel in human skeletal myotubes: an activation defect caused by the hypokalemic periodic paralysis mutation R528H. (1998) J Neurosci. 18 (24):10320–34.
22. Kuzmenkin A, Hang C, Kuzmenkina E, Jurkat-Rott K. Gating of the HypoPP-1 mutations: I. Mutant-specific effects and cooperativity. (2007) Pflügers Arch Eur J Physiol. 454(3):495–505.